https://doi.org/10.3311/PPci.36817

Periodica Polytechnica Civil Engineering

Influence of Key Shear Factors on the Shear Performance of Ultra-high Performance Fibre Reinforced Concrete Beam Containing Coarse Aggregate

Abutu Simon John Smith[1*], Gang Xu[1]

[1] College of Civil Engineering and Architecture, China Three Gorges University, 8 Daxue Road, 443002 Yichang, China
[*] Corresponding author, e-mail: abutusmith@gmail.com

Received: 08 March 2024, Accepted: 03 July 2024, Published online: 22 July 2024

Abstract

This paper assesses the effect of direct and indirect factors on the shear performance of ultra-high performance fibre reinforced concrete beam containing coarse aggregate (UHPFRC-CA) using four point loading arrangement. The obtained results were used to categorize UHPFRC-CA beam's failure mode, establish the influence of key factors on shear performance, and develop UHPFRC-CA beam's compression zone resistance and first shear cracking load equations whose results were compared with those from this research, other researchers and existing equation. Findings revealed that UHPFRC-CA beam fails in cable stayed, shear partial compression, cable stayed-diagonal tension and cable stayed-partial shear tension. Shear span-depth ratio (a/d) has the most influence on the beams' failure mode. Higher percentage volume of steel fibre improves ultimate load capacity and midspan displacement resistance at failure load. Hooked-end steel fibre improves deformation (crack width and midspan displacement at failure load) resistance. Higher a/d is more beneficial to midspan displacement resistance at failure load than load capacity; while lower stirrup spacing leads to higher midspan displacement at failure load. Finally, the developed first shear cracking load equation can adequately capture the true first shear cracking load of UHPFRC-CA beam; and the developed compression zone resistance equation can be conveniently used to represent the joint contribution of compressive strength and fibre factor to UHPFRC-CA beam's shear resistance.

Keywords

beam, coarse aggregate, compression zone resistance, shear cracking equation, shear factors, ultra-high performance fibre reinforced concrete

1 Introduction

The mechanical properties of ultra-high performance fibre reinforced concrete containing coarse aggregate (UHPFRC-CA) have been extensively studied [1–4] to establish the suitability of coarse aggregate in ultra-high performance fibre reinforced concrete (UHPFRC); and findings revealed that incorporating coarse aggregate in the mixture reduces hydration heat and minimizes the cost of producing UHPFRC. Several literatures [1–4] have also studied and recommended the type, particle size, particle type of coarse aggregate with the required moisture content, texture and shape to use in UHPFRC to give optimum mechanical performance; and this has helped researchers undertaking structural performance of UHPFRC-CA to carefully design UHPFRC-CA mix without considering material performance (including the percentage of coarse aggregate in the mix).

It is really hard at the moment to find literatures on the shear behaviour of UHPFRC-CA beams because researches on the structural performance of UHPFRC-CA members are still at the infant stage. Kodur et al. [5] studied the shear resistance of two UHPFRC-CA beams containing limestone coarse aggregate and found that the beams failed in shear with a single macro cracks at failure load. Unlike the limited researches on the shear performance of UHPFRC-CA beams, a lot of studies have been conducted on the shear behaviour of UHPFRC beams. For example, Hegger and Bertram's [6] findings on the shear capacity of UHPFRC beams showed that the use of 2.5% fibre volume content in a prestressed UHPFRC beam increased its shear capacity by 177%. Graybeal [7] opined that UHPFRC beam has a higher shear and flexural capacities when compared with a prestressed high

Cite this article as: Smith, A. S. J., Xu, G. "Influence of Key Shear Factors on the Shear Performance of Ultra-high Performance Fibre Reinforced Concrete Beam Containing Coarse Aggregate", Periodica Polytechnica Civil Engineering, 2024. https://doi.org/10.3311/PPci.36817

performance concrete I girder. Yoo and Yoon [8] reported that the inclusion of 2.5% steel fibre in UHPFRC beam increased its shear strength by about 250%. Maroliya [9] reported that steel fibres play significant role in arresting UHPFRC beam's cracks leading to the formation of many cracks with improved shear strength before the occurrence of failure. Xu and Deng [10] reported that prestressing UHPFRC beams also improve the shear cracking force and slows the growth of diagonal cracks. Xu et al. [11] opined that increase in shear reinforcement ratio leads to increase in UHPFRC beam's shear capacity. Ji et al. [12] found that the beam's failure mode is quite different from normal concrete. Jin et al. [13] reported that shear span-depth ratio (a/d) has the most influence on UHPFRC beam's shear capacity; while longitudinal reinforcement ratio (ρ) improves both shear capacity and shear ductility. Findings have also shown that steel fibre's percentage volume (V_f) of 2% has some significant effect on UHPFRC beam's shear capacity with the impact becoming insignificant as V_f is increased beyond 2% [14].

Several literatures [15–17] have focused more on the influence of steel fibre length (l_f), diameter (d_f), V_f and fibre bond factor (α) on UHPFRC beam's shear strength; and have paid little or no attention on how compressive strength (f_{cu}) influences shear strength. The resistance against shear load provided by any concrete compression zone is mainly dependent on that concrete strength and for better understanding of the internal failure mechanism of UHPFRC-CA beam, it is important to develop an equation to predict the contribution of compression zone resistance to shear strength. So far, it is hard to find equations developed for estimating the first shear cracking load of UHPFRC beams as most researchers and standards [18–21] only concentrate on developing equations for predicting the ultimate shear capacity of UHPFRC beams. Although Narayanan and Darwish [22] developed a shear cracking equation for steel fibre reinforced concrete (SFRC) beams, it yields higher values when employed for UHPFRC-CA/UHPFRC beams and this is technically bad for shear behaviour test; and hence calls for the development of a first shear cracking load equation for UHPFRC-CA/UHPFRC beams. This paper is therefore targeted at evaluating the effects of direct (steel fibre shape, V_f, a/d, stirrup spacing (s), presence/absence of stirrups) and indirect (f_{cu} and coarse aggregate) shear factors on UHPFRC-CA beam's shear behaviour in order to categorize the crack pattern and failure mode of UHPFRC-CA beam; establish UHPFRC-CA beam's resistance to shear loading, develop an equation for the contribution of compression zone resistance against shear load and to as well formulate the first shear cracking load equation for UHPFRC-CA beam.

2 Test program

The materials used were: P.O 52.5 (cement 1); P.C 42.5 (cement 2); straight steel fibre of 0.2 mm diameter, 13 mm length and 2850 N/mm^2 tensile strength; hooked-end steel fibre of 0.3 mm diameter, 22 mm length and 2850 N/mm^2 tensile strength; Quartz sand of ≤1 mm sieve size; gravel of size between 5 mm and 10 mm; silica fume; super plasticizer and portable water. The two cement types were used because of two reasons:

1. using only P.O 52.5 leads to increased heat of hydration but the introduction of P.C 42.5 reduces heat of hydration,
2. the introduction of coarse aggregate into the mix reduces workability of the concrete but the introduction of P.C 42.5 helps to increase the UHPFRC-CA's workability.

The addition of coarse aggregate into this mix was aimed at reducing drying shrinkage and creep, providing better resistance to crack propagation and widening of already developed cracks, and to see if midspan displacement at ultimate load can be minimized. Funk and Dinger [23] model was used to design the UHPFRC-CA mixes as presented in Table 1.

Beams with: 1200 mm length, 200 mm height, 100 mm breadth, 15 mm cover, ρ of 0.0373, tension steel of deformed 2∅20, compression steel of smooth 2∅6.5, stirrup steel of smooth 9∅6.5 were design for shear using Narayanan and Darwish [22] analytical equation. The UHPFRC-CA beams' longitudinal-cross sections are presented in Fig. 1. This study classified the beams into six classes (B1, B2, B3, B4, B5 and B6) as presented in Table 2 and divided

Table 1 Designed mix proportion

Materials	B(1-6)a, B1b, B3b, B4b, B5b	B2b	B6b
Cement 1	461.01	456.31	519.44
Cement 2	322.70	319.41	363.61
Fine aggregate	922.01	912.61	1038.89
Coarse aggregate	412.50	408.29	-
Silica fume	138.30	136.89	155.83
Steel fibres	133.45	200.18	156.00
Super plasticizer	22.50	22.27	20.78
Water	166.25	164.55	166.22

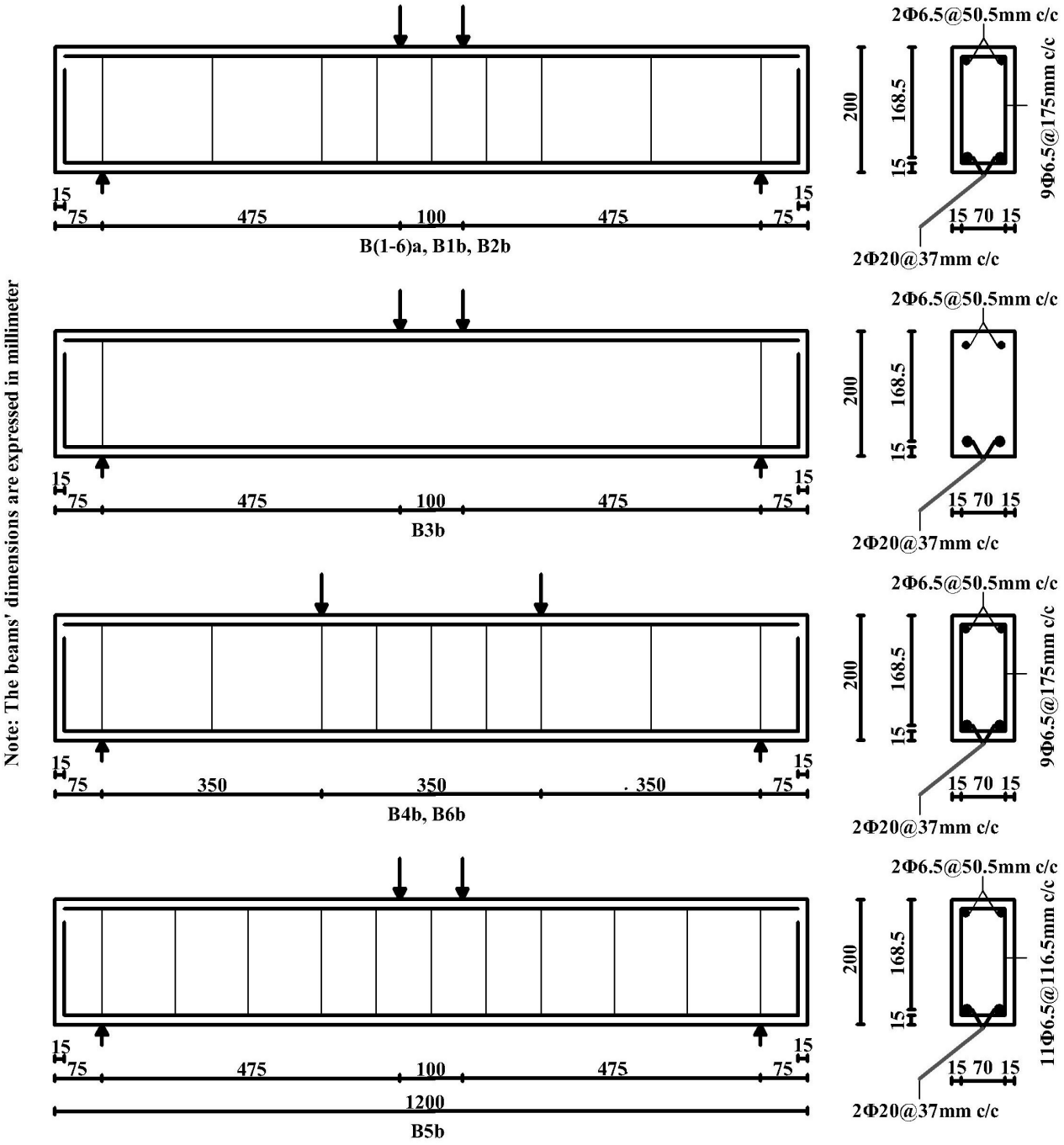

Fig. 1 UHPFRC-CA beam's longitudinal-cross section

each class into two levels for each shear design parameters. Twelve cube specimens of 100 mm^3 sizes were cast and tested for f_{cu} (see Table 3) based on CECS 13-2009 [24] to study the influence of f_{cu} on shear performance. Similarly, 12 dog-bone specimens with length of 368 mm, 50 mm × 80 mm × 100 mm end sections, 50 mm × 50 mm prismatic middle portion, tapered section of length 54 mm and radius of 70 mm, and a notched section of 100 mm length were cast and tested for uniaxial tension to determine the direct tensile strength and tensile stress-strain of the UHPFRC-CA based on T/CBMF 37-2018 [25] recommendation. 12 prismatic specimens were also cast using 100 mm × 100 mm × 300 mm mould to determine the elastic modulus of the UHPFRC-CA specimens in accordance with CECS 13-2009 [24] specification.

The beam shear test adopted the loading system of four-point concentrated force loading based on GB/T 50152-2012 [26] with the following modifications to suit

Table 2 Shear design parameters and f_{cu}

Beam class	Research parameters						
	Beam specimen	Steel fibre	V_f(%)	Stirrups	a/d	s (mm)	Coarse aggregate
B1	B(1-6)a	Straight	2	Yes	2.82	175	Yes
	B1b	Hooked-end	2	Yes	2.82	175	Yes
B2	B(1-6)a	Straight	2	Yes	2.82	175	Yes
	B2b	Straight	3	Yes	2.82	175	Yes
B3	B(1-6)a	Straight	2	Yes	2.82	175	Yes
	B3b	Straight	2	No	2.82	175	Yes
B4	B(1-6)a	Straight	2	Yes	2.82	175	Yes
	B4b	Straight	2	Yes	2.08	175	Yes
B5	B(1-6)a	Straight	2	Yes	2.82	175	Yes
	B5b	Straight	2	Yes	2.82	116.5	Yes
B6	B4b	Straight	2	Yes	2.08	175	Yes
	B6b	Straight	2	Yes	2.08	175	No

Table 3 Mechanical properties of the beam speciments

Beam	B(1-6)a, B1b, B3b, B4b, B5b	B1b	B2b	B6b
f_{cu} (N/mm^2)	154.6	142.4	165.2	166.8
Deviation of f_{cu} from designed f_{cu} of 150 N/mm^2 (%)	3.1	−5.1	10.1	11.2
f_t (N/mm^2)	5.5	5.3	5.5	6.1
Elastic modulus (N/m^2)	46875	40000	40000	43269

UHPFRC: Preloading was done using 5, 10 and 15 kN loads with readings taken at 0, 2.5th and 5th minute. After preloading, 15% of the calculated cracking load (P_{cr}) was continuously added to the load value of each loading steps until the applied load reached 75% of P_{cr}. Afterwards, the additional load value of each loading steps was changed to 5% of P_{cr}. When the specimen cracked, the additional load value of each loading steps became 10% of the calculated ultimate load (P_u) of the test beam; and this loading process was continued until the failure of the beam. The setup of the experiment is shown in Fig. 2.

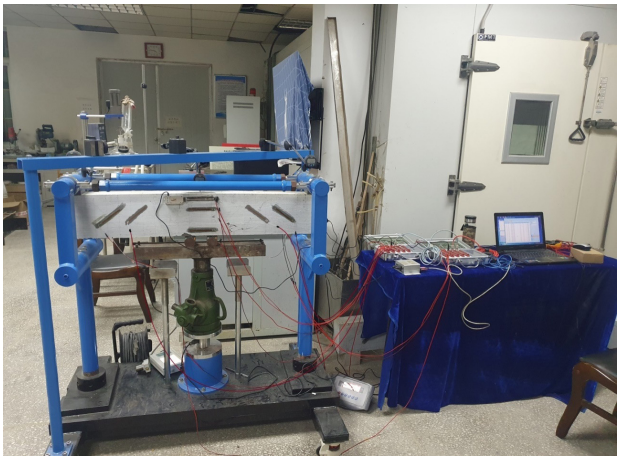

Fig. 2 Set up of the experiment

3 Results and discussions

3.1 Shear performance of the UHPFRC-CA beams

3.1.1 Failure pattern of the UHPFRC-CA beams

The UHPFRC-CA beams failed with lower diagonal crack widths when compared with similar ordinary UHPFRC beams in existing literatures [18, 21, 27]. This means that, as it is customary in ordinary UHPFRC beams to have widely opened diagonal cracks after attaining ultimate load due to reduced fibre participation in resisting shear stress, UHPFRC-CA beam, because of the hard nature of coarse aggregate in its mix, possessed the ability to prevent its diagonal cracks from having widely opened width after reaching ultimate load. UHPFRC-CA beams also underwent failure modes that are uniquely different from ordinary UHPFRC beams and its detailed discussion is in Section 3.1.3. The crack pattern and failure mode of the UHPFRC-CA/UHPFRC beams are shown in Fig. 3; while the flexural cracking load, first shear cracking load and main diagonal cracking load of the beams are presented in Table 4.

3.1.2 Effect of research parameters on the beams' crack pattern and failure mode

Steel fibre shape does not affect the total number of crack formation at the face of the beam where failure occurred; however, hooked-end shape changed the failure mode and the inclination angle of the main diagonal crack from 42° (B(1-6)a) to 53° (B1b). Hooked-end steel fibre exhibits better resistance to first crack appearance than straight steel fibre; and this may be due to the improved fibre-concrete matrix bond provided by its hooked end [28]. In comparison with ordinary UHPFRC beam with hooked-end steel fibre [28] whose

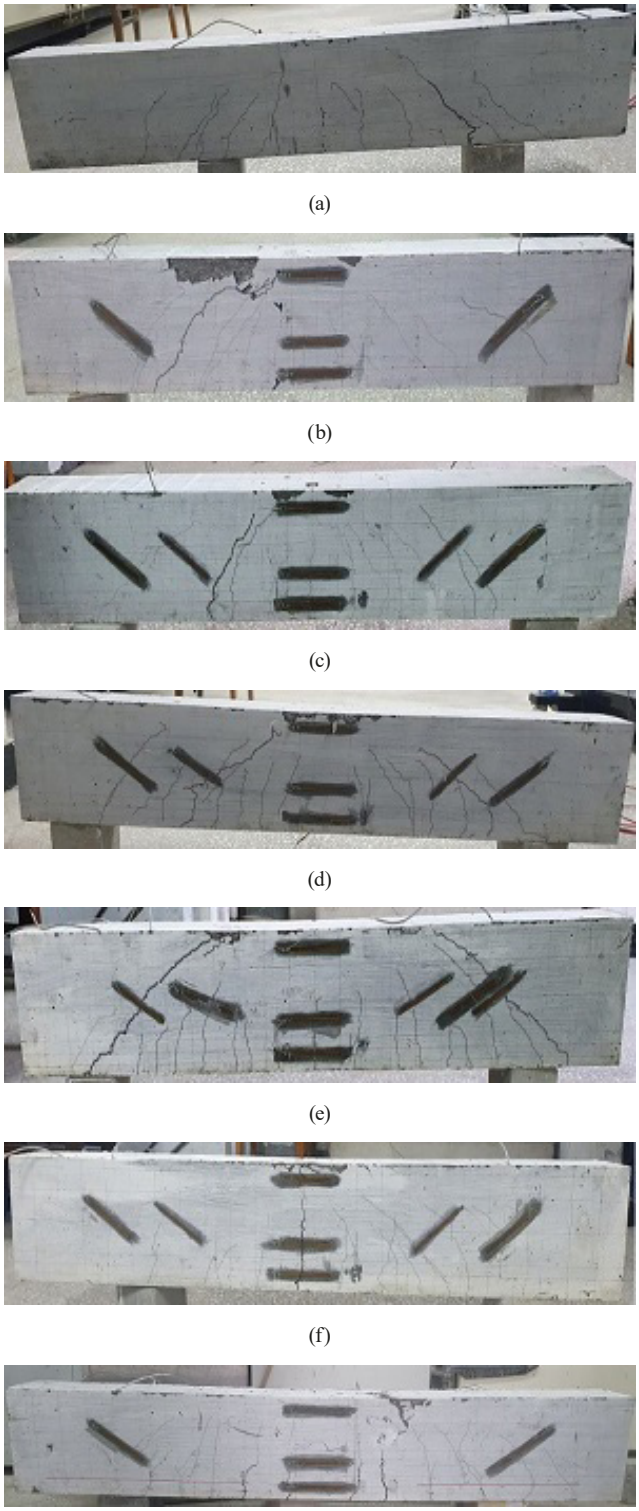

(a) (b) (c) (d) (e) (f) (g)

Fig. 3 UHPFRC-CA/UHPFRC beams' crack pattern and failure mode: (a) B(1-6)a, (b) B1b, (c) B2b, (d) B3b, (e) B4b, (f) B5b, (g) B6b

shear crack appeared between 17%–40% of its peak capacity, this UHPFRC-CA beam's shear crack appeared at ≤20% of its peak capacity; and this is due to the presence of coarse aggregate that makes it less packed than ordinary UHPFRC.

Table 4 Failure mode and cracking load of the beams

Beam	Failure mode	Flexural cracking load (kN)	Shear cracking load (kN)	Diagonal cracking load (kN)
B(1-6)a	Cable stayed-flexure	26	49	95
B1b	Cable stayed-diagonal tension	28	51	97
B2b	Cable stayed-diagonal tension	26	50	98
B3b	Cable stayed-partial shear tension	26	46	82
B4b	Shear partial compression	24	52	108
B5b	Flexure	26	54	-
B6b	Flexure	29	57	113

The number of cracks within the shear zone of the beam's face where failure occurred reduced with increase in V_f; and this behaviour is the same with that of ordinary UHPFRC beam [20]. The inclination angle of the diagonal crack also increased with increase in V_f from 42° (B(1-6)a) to 57° (B2b). There was also a change in failure from cable stayed-flexure to cable stayed-diagonal tension failure when the V_f was increased with the diagonal crack of the beam containing 3% V_f being closer to the loading point than the beam with 2%. This change in inclined strut angle and failure mode with increase in V_f can be attributed to the bridging mechanism of the extra steel fibre; and this was also reported by Hosamo and Sarwari [29] for ordinary UHPFRC beam.

The elimination of stirrups from B(1-6)a led to increased number of cracks in B3b, increase in the inclination angle of its diagonal crack from 42° to 53° and also changed the failure mode of the beam. This beam's crack pattern and mode of failure is due to the absence of stirrups to resist the tensile force build up in the beam's existing cracks which led to decrease in the beam's stiffness beyond its peak force [30]; as well as the mobilisation of dowel action along with some degree of concrete-tensile reinforcement bond failure [31]. This failure of the beam is a failure pattern that is common with ordinary UHPFRCs made without stirrups [5, 32]. This means that the elimination of stirrups from the UHPFRC-CA has a greater influence on the beam's failure mode than the presence of coarse aggregate; and this is why B3b exhibited the same behaviour like ordinary UHPFRC beam without stirrup. B3b's diagonal crack

nearly propagated through the whole depth of the beam unlike normal/high strength concrete without stirrups that will fail before reaching its ultimate strength [33].

As *a*/*d* of the beam was reduced from 2.82 (B(1-6)a) to 2.08 (B4b), the total number of cracks in the beam increased, its failure mode changed from cable stayed-flexure failure to shear partial compression failure, and the inclination angle of its diagonal crack increased from 42° to 45°. This change in failure mode of the beam with change in *a*/*d* is in line with the behaviour of ordinary UHPFRC beam as Bahij et al. [34] reported that the mode of failure of ordinary UHPFRC beams change from shear to almost flexure shear as the value of *a*/*d* increases.

The failure mode of the beam changed from cable stayed-flexure failure to pure flexure failure; and the distance between the developed diagonal cracks reduced when its s was reduced from 175 mm (B(1-6)a) to 116.5 mm (B5b). In ordinary UHPFRC beam [18], reduction in stirrup spacing does not lead to change in failure mode from shear to flexure but only leads to decrease in the spacing between diagonal cracks. So this behaviour of complete change in failure mode of UHPFRC-CA beam may not be due to the presence of coarse aggregate but due to the short length of the UHPFRC-CA beam as Ahmad et al.'s [18] beam is 800 mm longer than this UHPFRC-CA beam. Also, decrease in the beam's s resulted in lesser number of diagonal cracks with lesser crack width instead of wider crack width as reported by Bahij [20]. The lesser number of diagonal cracks may be attributed to the distribution of the applied load to a smaller area of the beam as a result of increase in the number of stirrups. While the lesser diagonal crack width instead of wider diagonal crack width is simply because the beam failed in flexure instead of shear. The presence of coarse aggregate in the beam changed the failure mode of the beam from pure flexure (B6b) to pure shear (B4b) and also resulted in increased number of cracks formed in the beam's failure face. The inclination angle of the main diagonal crack of B6b decreased from 66° to 45° when coarse aggregate was used as an ingredient.

3.1.3 Categorization of UHPFRC-CA beam's crack pattern and failure mode

The crack pattern resulting from the UHPFRC-CA beams' failure can be categorized into: single diagonal crack and double diagonal cracks. For a UHPFRC-CA beam whose length is not greater than 1200 mm, the beam is likely to fail from the formation of a single diagonal crack if the value of *a*/*d* is in the range of 2.1–2.82. When the value of *a*/*d* is less than 2.1, the beam's failure is as a result of the formation of double diagonal cracks. This study's UHPFRC-CA beams exhibit distinct failure modes that vary from ordinary UHPFRC beam. This unique failure mode is demonstrated in the UHPFRC-CA beams' ability to fail in a non-conventional way and in a way where existing failure modes are combined for a particular beam under shear loading. UHPFRC-CA beam under shear loading can be categorized into four main failure modes:

1. Cable stayed Failure: This failure mode occurs in UHPFRC-CA beams with stirrups when the diagonal crack has no vertical base from the tension zone of the beam. This means that the diagonal crack has no direct link to any initial vertical crack and it develops as an inclined crack within the beam's shear critical area and propagates towards the middle height of the beam. The diagonal crack of this failure mode hardly propagates to the extreme compression zone and may likely stop at a little distance above the beam's neutral axis. Fig. 4 (a) presents cable stayed failure.

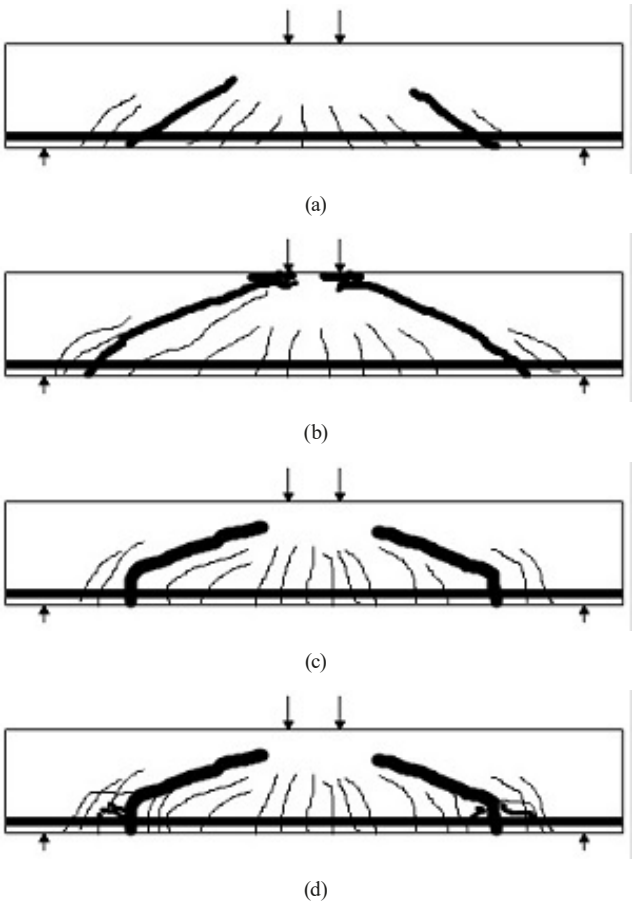

Fig. 4 Categorized failure modes of UHPFRC-CA beams: (a) Cable stayed failure, (b) Shear partial compression failure, (c) Cable stayed-diagonal tension failure, (d) Cable stayed-partial shear tension failure

2. Shear Partial Compression Failure: This failure mode has the same diagonal crack base like cable stayed failure but the difference is in the diagonal crack propagating beyond the middle height of the beam to the compression zone; causing the compression zone to experience slight concrete spalling at the beam's side and top of the compression fibre. This spalling may be due to the weakness in the UHPFRC-CA beam's matrix caused by the shear loading which is being resisted as UHPFRC-CA's ultra-high f_{cu} prevents the beam from undergoing shear compression in the compression zone. If the concrete spalling fails to occur, the failure mode can be simply called single or double shear diagonal failure. Shear partial compression failure is shown in Fig. 4 (b).
3. Cable Stayed-Diagonal Tension Failure: This failure mode is a bit related to UHPFRC beams and SFRC beams' failure in terms of the diagonal tension. In this failure mode, the UHPFRC-CA beam with stirrups first developed a vertical crack below the position of the tensile reinforcement and grows in width and propagates above the tension fibre to form a diagonal crack. The developed diagonal crack continues to propagate towards the load point and eventually leads to the UHPFRC-CA beam's failure as the loading continues. This category of failure mode may be common in UHPFRC-CA beams with >2% V_f in its mix. Fig. 4 (c) shows cable stayed-diagonal tension failure.
4. Cable Stayed-Partial Shear Tension Failure: This failure mode has all the features of cable stayed failure with the addition of few inter-connected short cracks around the diagonal crack along the tensile reinforcement location. This failure mode is likely to occur in UHPFRC-CA beams without stirrups in which the absence of stirrups causes extra shear stress to be borne or redistributed to the tensile steel reinforcement when diagonal crack develops in the beam. Fig. 4 (d) shows cable stayed-partial shear tension failure.

3.1.4 Load-midspan displacement performance of the UHPFRC-CA beams

Fig. 5 (a) revealed that all the beams have similar load-midspan displacement curve where their deformation occurred in linear and non-linear stages [35]. This deformation is also similar to that of ordinary UHPFRC beams as shown in Fig. 5 (b). The only difference being higher shear cracking load and ultimate load (due to lower packed density

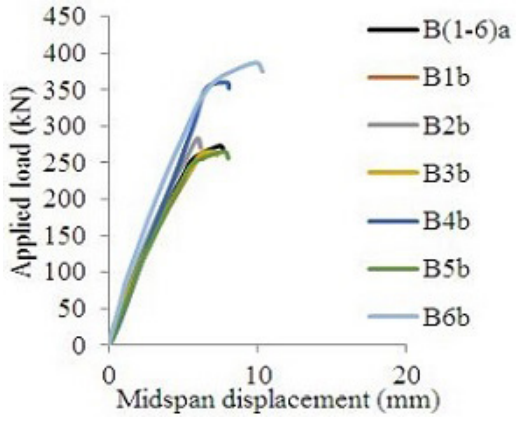

(a)

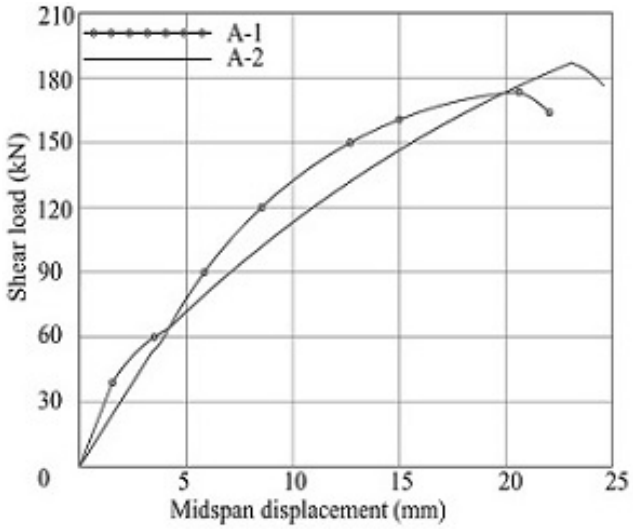

(b)

Fig. 5 Load-midspan displacements of the beams: (a) UHPFRC-CA beams, (b) Ahmad et al.'s [18] beam

of UHPFRC-CA beams because of coarse aggregate presence) for the ordinary UHPFRC beams (note that ultimate load = 2 × the shear load in Fig. 5 (b)); and lower midspan displacement (because of the hard nature of coarse aggregate in UHPFRC-CA beams that gives them extra rigidity to resist deformation) for the UHPFRC-CA beams. The ultimate load of B(1-6)a, B1b, B2b, B3b, B4b, B5b and B6b are 273 kN, 258 kN, 283 kN, 265 kN, 360 kN, 265 kN and 387 kN respectively with corresponding midspan displacement of 7.41 mm, 6.08 mm, 5.9 mm, 6.97 mm, 7.88 mm, 7.7 mm and 9.81 mm.

3.1.5 Effect of research parameters on the beams' load-midspan displacement

The load-midspan displacement of beams B(1-6)a (with straight steel fibre) and B1b (with hooked-end steel fibre) as illustrated in Fig. 5 (a) revealed that hooked-end

increased the beam's resistance to load application by 4% and reduced its resistance to midspan displacement by 12% at the phase of shear crack appearance; while at the ultimate load stage, hooked-end shape reduced the beam's resistance to applied load by 6% and improved its resistance to midspan displacement by 18%. The load-midspan displacement behaviour (at shear crack appearance phase and ultimate load phase) of this UHPFRC-CA beam with hooked-end shape was compared with Voo et al.'s [36] ordinary UHPFRC beam; and it was observed that both beams have the same behaviour. However, at the phase of first shear crack appearance where B1b has higher load than B(1-6)a, ordinary UHPFRC beam with hooked-end shape has lower load than that with straight steel fibre; and this may be due to the coarse aggregate's role in minimizing the growth and propagation of existing crack. This is true because flexural cracks usually appear first during UHPFRC-CA beam's shear test and the development of shear crack mostly emanate from the propagation of the flexural crack. So if coarse aggregate's presence minimizes the propagation of already existing flexural cracks, the load at which the first shear crack will appear in the UHPFRC-CA beam will eventually be higher. This means that the improved fibre-matrix interaction of the beam through hooked-end steel fibre only had direct impact on the cracking load and ultimate midspan displacement of the beam as its ultimate load was lower than the beam made with straight steel fibre. This lower ultimate load may be due to indirect influence of the beam's f_{cu}.

V_f increase from 2% to 3% increased the shear cracking load by 2% and reduced the midspan displacement by 5% at the appearance of the first shear crack; while at the ultimate load phase, the load capacity was increased by 4% and the midspan displacement was reduced by 20%. The ultimate load increment was a direct effect of the increase in steel fibre which tends to hold the beam's crack walls together as reported by other researchers [28, 37]. Even though the strength increase was not high when V_f was increased, this study has shown that high content of steel fibre greatly improved the resistance of UHPFRC-CA beam to midspan displacement. In an existing study on ordinary UHPFRC beam [18], 1% increase in V_f, resulted in 8% and 10% increment in ultimate load and midspan displacement respectively. The load capacity behaviour of the ordinary UHPFRC beam is comparable with this UHPFRC-CA beam's behaviour while the midspan displacement behaviour is completely different from this UHPFRC-CA beam. The reason why the UHPFRC-CA beam has better resistance to midspan displacement than the ordinary UHPFRC beam is because the coarse aggregate inclusion in the UHPFRC-CA beam acted as another hard UHPFRC-CA material that provided extra rigidity against the beam's deflection at the middle.

Stirrup exclusion from the UHPFRC-CA beam resulted in 6% and 4% reduction in load capacity and midspan displacement respectively at the stage of first shear crack development; while at ultimate load phase, the load capacity and midspan displacement decreased by 3% and 6% respectively. In ordinary UHPFRC beams, the elimination of stirrups also have no serious influence on the ultimate load of the UHPFRC beam as reported by Baby et al. [27]. This high load capacity exhibited by the UHPFRC-CA beam without stirrups may come from the additional diagonal cracks that helped in redistributing internal stresses within the internal structure of the beam [31]; while the increased resistance to midspan displacement is caused by the high shear stiffness of the UHPFRC-CA beam [38]. Analysis of this UHPFRC-CA beam without stirrups also revealed that there was only slight reduction in the ultimate load of the beam; which means that other factors must have indirectly contributed to the shear resistance of the beam. One of these factors may be the concrete f_{cu} as the beam with stirrups and that without stirrups both have the same f_{cu} of 154.6 N/mm^2. So its high shear resistance can be attributed to the combined contribution of high f_{cu} and the bridging mechanism of steel fibre.

B4b with *a*/*d* ratio of 2.08 at the time of shear crack appearance has 6% and 35% higher applied load and midspan displacement respectively than B(1-6)a with *a*/*d* ratio of 2.82; while at ultimate load stage, its applied load and midspan displacement increased by 32% and 6% respectively. The ultimate load of UHPFRC-CA beam decreased with increase in *a*/*d* and this performance characteristic is in agreement with existing literatures [39, 40] on ordinary UHPFRC. This ultimate load reduction when the value of *a*/*d* is increased may be caused by the developed compound tensile stress in the beam's critical region which combined with the beam's bending moment to form diagonal crack at lower load value. With B4b and B(1-6)a having the same properties and shear parameters except *a*/*d*, it can be conveniently put that *a*/*d* has a direct influence on the shear capacity of the UHPFRC-CA beam. This type of UHPFRC-CA beam with *a*/*d* of 2.08 is classified under short beams and it is naturally expected to fail in shear

tension at the anchorage or shear compression through concrete crushing like normal concrete beams however, it has high tensile resilience and ultra-high f_{cu} like ordinary UHPFRC beams that only favours failure through diagonal failure. So this UHPFRC-CA beam behaved in a similar way to ordinary UHPFRC beam when the *a*/*d* was reduced.

The reduction of s from 175 mm to 116.5 mm caused 3% decrease in the UHPFRC-CA beam's ultimate load and 4% increase in its midspan displacement. This ultimate load reduction with decrease in stirrup spacing of the UHPFRC-CA beam is an opposite performance characteristic when compared with ordinary UHPFRC [18, 34] but the reason for this behaviour is because the beam failed in flexure and not in shear. The increased midspan displacement as the stirrup spacing was reduced may be due to the distribution of the applied load over a small area available within two stirrups. The inclusion of coarse aggregate in UHPFRC mix resulted in 9% decrease in applied load and 49% increase in midspan displacement at the appearance of shear crack in the beam; while at the ultimate load phase, the applied load and midspan displacement of the beam reduced by 7% and 20% respectively. The ultimate load of the UHPFRC-CA beam (B4b) is less than that of the UHPFRC (B6b) probably because the steel fibre was unable to overlay the coarse aggregate due to its size unlike when UHPFRC contains only fine aggregates [2]. The UHPFRC-CA has lower midspan displacement because coarse aggregate provided extra shear stiffness to the beam to resist midspan displacement [38].

3.1.6 Effect of coarse aggregate on elastic modulus, compressive strength and tensile stress-strain; and their relationship to the UHPFRC-CA beams' shear load

Table 3 showed that the elastic modulus of UHPFRC-CA with coarse aggregate (B4b) was 8% higher than the UHPFRC without coarse aggregate (B6b); and this increased elastic modulus resulted in 9% and 8% decrease in shear cracking load and ultimate load respectively of the UHPFRC-CA beam under shear loading. Aso, there was 15% decrease in both the elastic modulus of UHPFRC-CA with hooked-end steel fibre (instead of straight steel fibre) and 3% straight steel fibre (instead of 2%). Further analysis of Table 3 showed that the 7% decrease in ultimate compressive strength (f_{cu}) of the UHPFRC (B6b) on addition of coarse aggregate to produce UHPFRC-CA (B4b) also translated to 5 kN decrease in shear cracking load and 27 kN decrease in the ultimate load of the UHPFRC-CA beam.

Fig. 6 revealed that the inclusion of coarse aggregate into the UHPFRC (B6b) to make UHPFRC-CA (B4b) resulted in 9.8% and 22.2% decrease in the ultimate tensile strength (f_t) and ultimate tensile strain respectively. Fig. 6 also showed that UHPFRC-CA with straight steel fibre (B4b) has 3.6% higher ultimate tensile strength than UHPFRC-CA with hooked-end steel fibre (B1b). The ultimate tensile strength of the UHPFRC-CA (B4b) with 2% straight steel fibre was not affected when it was increased to 3%. As the ultimate tensile strength of the UHPFRC (B6b) decreased as a result of coarse aggregate inclusion (B4b), the beam's shear cracking load and ultimate load also decreased by 9% and 8% respectively.

3.2 Formulation of compression zone resistance equation and first shear cracking load equation

3.2.1 Compression zone resistance equation

This compression zone resistance equation can also be described as shear strength-f_{cu}/fibre factor (F_f) term. The analysis of the effect of research parameters on the beams' load-midspan displacement discussed in Section 3.1.5 showed that the f_{cu} of the UHPFRC-CA must have influenced the ultimate load or shear strength of beams B1b and B3b. Most researchers ignore the influence of f_{cu} on the shear strength of UHPFRC (and focus more on steel fibre parameters like V_f, l_f and d_f) because it is not a direct shear influencing factor but based on the difference in ultimate load behaviour between B1b and B(1-6)a with different type of steel fibre (of which B1b according to literatures should have had higher ultimate load than B(1-6)a) and between B3b and B(1-6)a with the same parameters except stirrup (and only had small difference in ultimate

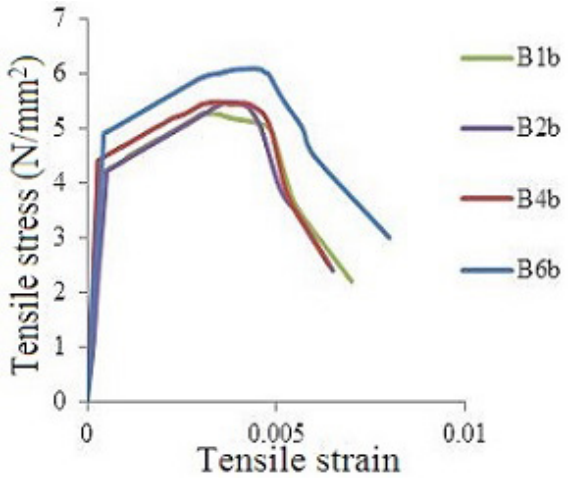

Fig. 6 Tensile stress-strain of the UHPFRC-CAs/UHPFRC

load), it is important to develop an analytical model that combines the joint effect of F_f and f_{cu} on the shear strength of UHPFRC-CA/UHPFRC beams. So, the contribution to the shear strength of the UHPFRC-CA beam from the combination of steel fibre and f_{cu} of the UHPFRC-CA cube specimen is hence termed $F_{cu/sf}$ (i.e. the force contribution of f_{cu} and F_f in resisting the applied shear load). The l_f, d_f, V_f and α have been reported in literatures [15–17] to have great effects on UHPFRC beam's shear strength; and have been modelled into Eq. (1) as F_f. According to Narayanan and Darwish [22], α for round, crimped and indented steel fibres are 0.5, 0.75 and 1.0 respectively.

$$F_f = \frac{l_f}{d_f} \times V_f \times \alpha \tag{1}$$

The respective F_f (0.65, 0.733 and 0.975) and f_{cu} (154.6, 142.4 and 165.2 N/mm^2) of B(1-6)a, B1b and B2b were utilized to model the contribution of F_f and f_{cu} to the shear strength (V_u) of UHPFRC-CA beam as presented in Fig. 7 (a) and Fig. 7 (b). Fig. 7 (a) being a quadrilateral curve and Fig. 7 (b) being a linear curve based on Smith and Sam [41] were used to formulate the compression zone resistance equation represented by $F_{cu/sf}$ as in Eq. (2):

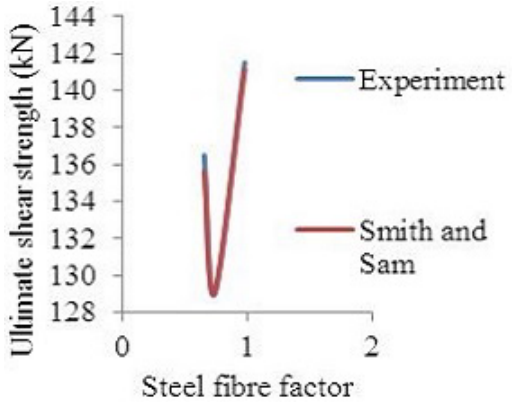

(a)

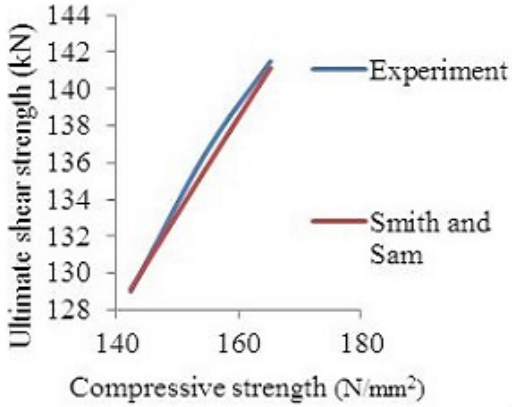

(b)

Fig. 7 Shear strength - F_f/f_{cu} relationship: (a) Shear strength - F_f curve, (b) Shear strength - f_{cu} curve

$$F_{cu/sf} = \left[Q\left(F_f\right)^2 - R\left(F_f - f_{cu}\right) + 2S \right] A_c , \tag{2}$$

where Q, R and S are constants determined as 0.1, 0.53 and 27 respectively using regression analysis; A_c is area of the beam (i.e. breadth x height (bh)).

The constants in Eq. (2) were replaced with their numerical values and expressed as:

$$F_{cu/sf} = \left[0.1F_f^2 - 0.53\left(F_f - f_{cu}\right) + 54 \right] A_c . \tag{3}$$

The effectiveness and detail validation of Eq. (3) is extensively carried out in Section 3.2.2 where it was utilized to propose the first shear cracking load equation for UHPFRC-CA beams.

3.2.2 First shear cracking load equation

The analysis of the first shear cracking load in UHPFRC-CA/UHPFRC beams is important because it gives researchers the idea on how to readjust the loading step (based on experimental procedures) during experiment of UHPFRC-CA/UHPFRC beams subjected to shear loading. Also, the two most important stages where the performance of a structural member undergoing shear loading is usually evaluated are the shear cracking load stage and ultimate load stage; and if the shear cracking load of UHPFRC-CA/UHPFRC beam is not correctly determined, any experimental result (midspan deflection, crack width, crack angle, strains, number of cracks, etc.) reported at shear cracking load phase will be wrong. So far, it is hard to find equations developed for estimating the shear cracking load of UHPFRC beams as most researchers [18–21] only concentrate on developing equations for predicting the ultimate shear capacity of UHPFRC beams. This means that there is no guarantee at all in knowing the true first shear cracking load of a UHPFRC-CA/UHPFRC beam, as there is no estimated value that can be used to guide researchers in readjusting the loading through small percentage increments when the loading is close to the estimated shear cracking load. It is therefore very important during experiment to have an estimated first shear cracking load to help researchers to obtain the correct performance of UHPFRC-CA beam at the right shear cracking load phase.

This analysis is based on the internal shear mechanisms that contributed the most in resisting shear load applied to UHPFRC-CA/UHPFRC beams before crack appearance.

There are three internal shear mechanisms (UHPFRC-CA compression zone, aggregate interlock and dowel action) that resist shear load application in UHPFRC-CA beam before crack appearance. Critical analysis of the load difference between B4b and B6b at first crack appearance showed a 5 kN difference (a difference that is significant because it is more than the load increment of 2 kN at the loading stage before crack appearance). This means that the influence of coarse aggregate in form of aggregate interlock contribution to the internal shear mechanism before crack appearance is significant and a coarse aggregate parameter in terms of maximum aggregate size (d_{ca}) has to be included when formulating this first shear cracking load equation. Since the cracking load of B4b with coarse aggregate was lower than B6b without coarse aggregate, the force contribution of coarse aggregate ($d_{ca}A_c$) represented as (F_{ca}) must carry subtraction sign in the equation. Also, to account for the fact that UHPFRC-CA with larger aggregate size have lower ultimate load than UHPFRC-CA with smaller aggregate size, the coarse aggregate parameter ($d_{ca}A_c$) must carry an inverse coefficient (Z^{-1}). So the force contribution of coarse aggregate to the cracking resistance of UHPFRC-CA beam is expressed as:

$$F_{ca} = -Z^{-1} d_{ca} A_c . \tag{4}$$

Dowel action contribution to the internal shear mechanism has been reported by several researchers [5, 20, 42] and have opined that dowel action (represented as F_d) contribution can be expressed as:

$$F_d = \left(\rho \frac{d}{a} \right) A_c . \tag{5}$$

For the UHPFRC-CA compression zone's contribution to the internal shear mechanism, the factors controlling this contribution are the f_{cu} and steel fibre. Steel fibre's contribution at this stage is only provided through F_f and not fibre pull out as fibre pull out strength only comes to play during post cracking behaviour. So, the UHPFRC-CA compression zone's contribution to the internal shear mechanism before crack appearance can be evaluated using Eq. (3). Narayanan and Darwish [22] developed an equation in the past for estimating the shear cracking load of SFRC beams and the predicted loads were in good agreement with the experimental loads. Narayanan and Darwish equation, when employed for estimating the shear cracking load of UHPFRC-CA/UHPFRC yielded higher values and this is technically bad for such delicate property during shear behaviour test. These higher values when used to calibrate the load increment in this loading stage may result in the determination of higher shear cracking load which may not be the true shear cracking load of the beam. The reason why Narayanan and Darwish equation predicted higher values of shear cracking load may be due to one or all of the following:

1. use of SFRC's f_{cu} in formulating the compression zone contribution to the resistance of shear crack appearance,
2. over representation of F_f in the equation,
3. use of SFRC beams parameters in determining the constants in the equation.

So Narayanan and Darwish equation as expressed in Eq. (6) was modified to develop the first shear cracking load equation for UHPFRC-CA/UHPFRC beam.

$$V_{cs} = \left[0.24 \left(\frac{f_{cu}}{20 - \sqrt{F_f}} + 0.7 + \sqrt{F_f} \right) + 20\rho \frac{d}{a} + 0.5F_f \right] bh \tag{6}$$

Equation (6) can be said to comprise three different parts: Part A is the compression zone part represented by $0.24\left(f_{cu} \Big/ \left(20 - \sqrt{F_f} \right) + 0.7 + \sqrt{F_f} \right)$ and will be replaced with this UHPFRC-CA's compression zone contributing force ($F_{cu/sf}$) presented earlier in Eq. (3). Part B is the dowel action factor represented by $20\rho d/a$ and this will not be changed in the new equation. Part C is the extended F_f represented by $0.5F_f$ which will also remain unchanged in the new equation. So, the modified Narayanan and Darwish equation is expressed as:

$$V_{cs} = \begin{bmatrix} 0.24\left(0.1F_f^2 - 0.53\left(F_f - f_{cu} \right) + 54 \right) \\ +20\rho \frac{d}{a} + 0.5F_f - Z^{-1} d_{ca} \end{bmatrix} bh . \tag{7}$$

Since the coefficients (0.24, 20 and 0.5) in Eq. (7) were determined by Narayanan and Darwish using SFRC beams' parameters and properties, they will be replaced with constants (L, M and N) as shown in Eq. (8) and re-determined using these UHPFRC-CA beams parameters.

$$V_{cs} = \begin{bmatrix} L\left(0.1F_f^2 - 0.53\left(F_f - f_{cu} \right) + 54 \right) \\ +M\rho \frac{d}{a} + NF_f - Z^{-1} d_{ca} \end{bmatrix} bh \tag{8}$$

The constants (L, M, N, and Z) were determined using excel solver through best-fitting the experimental data of the UHPFRC-CA beams presented in Table 5 to give Eq. (9).

Table 5 Experimental data for best-fitting of the developed V_{cs} equation

Beams	f_{cu} (N/mm^2)	F_f
B(1-6)a	154.6	0.65
B1b	142.4	0.733
B2b	165.2	0.975
B3b	154.6	0.65
B4b	154.6	0.65
B5b	154.6	0.65
B6b	166.8	0.65

$$V_{cs} = \begin{bmatrix} 0.017\left(0.1F_f^2 - 0.53\left(F_f - f_{cu}\right) + 54\right) \\ +14.2\rho\frac{d}{a} + 0.01F_f - 1000^{-1}d_{ca} \end{bmatrix} bh \quad (9)$$

The first shear cracking load equation developed in Eq. (9) was validated by comparing its results with this research's experimental results, results obtained using Narayanan and Darwish [22] equation and experimental results from existing literatures. The beams from literatures used for this validation include: Beam A2 from Ahmad et al.'s [18] research; beam BS-100-2.0 from Son et al.'s [32] study; beams SB2 and SB5 from Voo et al.'s [36] investigation; beams X-B7 and X-B8 from Voo et al.'s [43] research. The variables of the different beams used in validating Eq. (9) are presented in Table 6 and the results predicted using the new equation are shown in Table 7.

The first shear cracking load estimated using the developed equation as observed in Table 7 showed a fair degree of accuracy when compared with the experimental results from this study's beams, experimental results from other researchers' beams and results predicted using Narayanan and Darwish equation. The widest deviation of V_{cs} predicted by the developed equation was 11% and this occurred because the beam's (X-B7) f_{cu} was lower than the minimum UHPFRC-CA/UHPFRC's f_{cu} of 150 N/mm^2. On comparison of the new equation's predicted values with Narayanan and Darwish equation's predicted values, it can be clearly seen that the developed equation has much lower deviations (except for BS-100-2.0 and X-B8) than Narayanan and Darwish equation. The reason why Narayanan and Darwish had lower deviations for beams BS-100-2.0 and X-B8 is because those beams have lower f_{cu} like SFRC beams that Narayanan and Darwish equation was specifically proposed to predict. On a general scale, the newly developed equation performed better than Narayanan and Darwish equation as it has all round lower deviations from the experimental values with the widest deviation of 11% unlike Narayanan and Darwish whose deviation was as wide as 30%. Narayanan and Darwish estimations were mostly higher than the experimental values and this is not technically good as it can lead to experimental error of missing out on getting the true first shear cracking load of the UHPFRC-CA/UHPFRC beam.

It should be noted that the use of this developed first shear cracking load equation is at the moment limited to the thirteen sample beams from this study's experiment and existing literatutres; and there is need for the validation of more samples from existing/future literatures in order to increase its reliability. The reason why only thirteen beam samples were used for this validation is because one or more parameter values needed to evaluate the first shear cracking load of the beams in most existing literatures were not reported due to the negligence of first shear

Table 6 Variables used in estimating the different beams' first shear cracking load

Beams	f_{cu} (N/mm^2)	F_f	ρ	d (mm)	a (mm)	b (mm)	h	d_{ca} (mm)
B(1-6)a	154.6	0.65	0.0373	168.5	475	100	200	10
B1b	142.4	0.733	0.0373	168.5	475	100	200	10
B2b	165.2	0.975	0.0373	168.5	475	100	200	10
B3b	154.6	0.65	0.0373	168.5	475	100	200	10
B4b	154.6	0.65	0.0373	168.5	350	100	200	10
B5b	154.6	0.65	0.0373	168.5	475	100	200	10
B6b	166.8	0.65	0.0373	168.5	475	100	200	10
A2	150	0.59	0.01935	182.5	328.5	150	225	0
BS-100-2.0	100	0.4	0.032	300	600	200	350	0
SB2	178	0.8125	0.0134	620	2000	250	650	0
SB5	187	0.75	0.0134	620	2000	250	650	0
X-B7	122	0.75	0.00335	620	1550	500	650	0
X-B8	122	0.375	0.00335	620	1085	500	650	0

Table 7 Estimation of the first shear cracking load of UHPFRC-CA/UHPFRC beams

Beam	V_{cs} (kN)			*P*'s Deviation (%)	*N*'s Deviation (%)
	Experiment (*E*)	Present equation (*P*)	Narayanan and Darwish (*N*)		
B(1-6)a	49	47	59	−4	20
B1b	51	48	56	−6	10
B2b	50	52	65	4	30
B3b	46	50	59	9	28
B4b	52	52	60	−2	15
B5b	54	50	59	−7	9
B6b	57	52	62	−9	9
A2	78	82	94	5	21
BS-100-2.0	153	144	150	−6	−2
SB2	400	422	509	6	27
SB5	400	432	518	8	30
X-B7	600	667	758	11	26
X-B8	700	667	694	−5	−1

cracking load equation by researchers. However extra efforts were also made to validate the equation by comparing its predicted results with an existing equation for estimating the first shear cracking load of SRFC beam; and the results were promising. So this newly developed equation can be used to adequately predict the first shear cracking load of UHPFRC-CA/UHPFRC beams whose f_{cu} ranges from 150 N/mm^2 to 190 N/mm^2.

4 Conclusions

This research investigates the shear performance of UHPFRC-CA beam using steel fibre shape, V_f, a/d, s, presence/absence of stirrups and type of UHPFRC as experimental parameters. It also utilized the study's f_{cu}, first shear cracking load and F_f data to propose two equations for estimating UHPFRC-CA beam's compression zone resistance and first shear cracking load. The conclusions deduced from this investigation are as follow:

- UHPFRC-CA beams exhibit four distinct and unique failure mode of cable stayed failure, shear partial compression failure, cable stayed-diagonal tension failure and cable stayed-partial shear tension failure with the formation of many micro cracks and a major diagonal crack which usually causes failure.
- The shapes of steel fibre, V_f, a/d and stirrup spacing have great influences on the shear failure mode of UHPFRC-CA beams. The a/d is the most influential factor that affects the failure mode of UHPFRC-CA beam; and for UHPFRC-CA beams with the same a/d values, f_{cu} is the main factor that determines the type of cable stayed failure.
- UHPFRC-CA beam's performance in terms of deformation under four points loading configuration is both elastic and plastic deformation; and hooked-end steel fibre is the most influential shear factor that improves its deformation resistance (in terms of crack width and midspan displacement at failure).
- The ultimate load capacity and the corresponding midspan displacement resistance of UHPFRC-CA beam improved with increase in V_f; and the absence of stirrups in UHPFRC-CA beam has no significant influence on the beam's ultimate load.
- A higher value of a/d ratio leads to lower values of the beam's ultimate load and midspan displacement. Lower stirrup spacing leads to higher midspan displacement and changed UHPFRC-CA beam's failure mode from shear to flexure.
- Coarse aggregate in UHPFRC-CA prevents structural beams from undergoing excessive deformation (in terms of crack width and midspan displacement at failure) even after attaining its ultimate strength; and it also greatly minimises the growth rate of crack width when structural beams' applied load increased from one loading stage to another.
- The newly formulated first shear cracking load equation has the capability of adequately capturing the true first shear cracking load of UHPFRC-CA beam; and the developed equation for the joint contribution of f_{cu} and F_f to UHPFRC-CA beam's shear resistance can be conveniently used to represent the contribution of UHPFRC-CA's compression zone to shear resistance.

References

[1] Yujing, L., Wenhua, Z., Fan, W., Peipei, W., Weizhao, Z., Fenghao, Y. "Static mechanical properties and mechanism of C200 ultra-high performance concrete (UHPC) containing coarse aggregates", Science and Engineering of Composite Materials, 27(1), pp. 186–195, 2020. https://doi.org/10.1515/secm-2020-0018

[2] Li, P. P., Yu, Q. L., Brouwers, H. J. H. "Effect of coarse basalt aggregates on the properties of ultra-high performance concrete (UHPC)", Construction and Building Materials, 170, pp. 649–659, 2018. https://doi.org/10.1016/j.conbuildmat.2018.03.109

[3] Ma, J., Orgass, M., Dehn, F.,Schmidt, D., Tue, N. V. "Comparative investigations on ultra-high performance concrete with or without coarse aggregates", In: Proceedings of the International Symposium on Ultra-High Performance Concrete, Kassel, Germany, 2004, pp. 205–212. ISBN 3-89958-086-9

[4] Liu, S., Zhang, Y. "Static mechanical properties and microscopic analysis of hybrid fiber reinforced ultra-high performance concrete with coarse aggregate", Advances in Civil Engineering, 2022(1), 4529993, 2022. https://doi.org/10.1155/2022/4529993

[5] Kodur, V., Solhmirzaei, R., Agrawal, A., Aziz, E. M., Soroushian, P. "Analysis of flexural and shear resistance of ultra-high performance fiber reinforced concrete beams without stirrups", Engineering Structures, 174, pp. 873–884, 2018. https://doi.org/10.1016/j.engstruct.2018.08.010

[6] Hegger, J., Bertram, G. "Shear carrying capacity of ultra-high performance concrete beams", In: Walraven, J. C., Stoelhorst, D. (eds.) Tailor made concrete structures, CRC Press, 2008, pp. 341–347. ISBN 9780429103605 https://doi.org/10.1201/9781439828410.ch59

[7] Graybeal, B. A. "Material property characterization of ultra-high performance concrete", Office of Infrastructure Research and Development, Federal Highway Administration, McLean, VA, USA, Rep. FHWA-HRT-06-103, 2006.

[8] Yoo, D.-Y., Yoon, Y.-S. "A review on structural behaviour, design, and application of ultra-high-performance fiber-reinforced concrete", International Journal of Concrete Structures and Materials, 10(2), pp. 125–142, 2016. https://doi.org/10.1007/s40069-016-0143-x

[9] Maroliya, M. K. "Behaviour of reactive powder concrete in direct shear", IOSR Journal of Engineering (IOSRJEN), 2(9), pp. 76–79, 2012. https://doi.org/10.9790/3021-02917679

[10] Xu, H., Deng, Z. "Shear cracking force and diagonal crack width of UHPC beams", Sichuan Building Science, 43(4), pp. 12–15, 2017. (in Chinese)

[11] Xu, H., Deng, Z., Chen, C., Chen, X. "Experimental study on shear strength of ultra-high performance fibre reinforced concrete beams", China Civil Engineering Journal, 47(12), pp. 91–97, 2014. (in Chinese)

[12] Ji, W., Ding, B., An, M. "Experimental study on the shear capacity of reactive powder concrete T-beams", China Railway Science, 32(5), pp. 38–42, 2011. (in Chinese)

[13] Jin, L., Li, Y., Qi, K., He, P. "Research on shear bearing capacity and ductility of high strength reinforced RPC beam", Engineering Mechanics, 32, pp. 209–214,225, 2015. (in Chinese) https://doi.org/10.6052/j.issn.1000-4750.2014.04.S056

[14] Jin, L., Zhou, J., Li, Y., Cao, X., Fu, Q. "Experimental study on shear bearing capacity of RPC beams with high strength reinforcement", Journal of Building Structures, 36(S2), pp. 277–285, 2015. (in Chinese)

[15] Hashim, D. T., Hajezi, F., Lei, V. Y. "Simplified constitutive and damage plasticity models for UHPFRC with different types of fiber", International Journal of Concrete Structures and Materials, 14(1), 45, 2020. https://doi.org/10.1186/s40069-020-00418-9

[16] Yoo, D.-Y., Lee, J.-H., Yoon, Y.-S. "Effect of fiber content on mechanical and fracture properties of ultra-high performance fiber reinforced cementitious composites", Composite Structures, 106, pp. 742–753, 2013. https://doi.org/10.1016/j.compstruct.2013.07.033

[17] Aydın, S., Baradan, B. "The effect of fiber properties on high performance alkali-activated slag/silica fumes mortars", Composite Part B: Engineering, 45(1), pp. 63–69, 2013. https://doi.org/10.1016/j.compositesb.2012.09.080

[18] Ahmad, S., Bahij, S., Al-Osta, M. A., Adekunle, S. K., Al-Dulaijan, S. U. "Shear behaviour of ultra-high performance concrete beams reinforced with high-strength steel bars", ACI Structural Journal, 116(4), pp. 3–14, 2019. https://doi.org/10.14359/51714484

[19] AFNOR "NF P 18-710 National addition to Eurocode 2-Design of concrete structures: specific rules for ultra-high performance fibre reinforced concrete (UHPFRC)", AFNOR, Saint-Denis, France, 2016.

[20] Bahij, S. "Study on shear behaviour of ultra-high performance concrete (UHPC) beams", MSc Thesis, King Fahd University of Petroleum and Minerals, 2016.

[21] Hussein, L. "Structural behaviour of ultra-high performance fibre reinforced concrete composite members", PhD Dissertation, Ryerson University, 2015. https://doi.org/10.32920/ryerson.14668671.v1

[22] Narayanan, R., Darwish, I. Y. S. "Use of steel fibers as shear reinforcement", ACI Structural Journal, 84(3), pp. 216–227, 1987. https://doi.org/10.14359/2654

[23] Funk, J. E., Dinger, D. R. "Predictive process control of crowded particulate suspensions: Applied to ceramic manufacturing", Kluwer Academic Publishers, 1994. ISBN 978-0-7923-9409-9 https://doi.org/10.1007/978-1-4615-3118-0

[24] CECS "CECS 13-2009 Standard test methods for fiber reinforced concrete", China Association for Engineering ConstructionStandardization, Beijing, China, 2009. [online] Available at: https://www.doc88.com/p-91773113625122.html (in Chinese)

[25] CBMF "T/CBMF 37-2018 Fundamental characteristics and test methods of ultra-high performance concrete" China Building Materials Federation, Beijing, China, 2018. [online] Available at: https://www.doc88.com/p-58139740621068.html (in Chinese)

[26] GB "GB/T 50152-2012 Standard for test method of concrete structures", National Standard of the People's Republic of China, Shenzhen, China, 2012.

[27] Baby, F., Marchand, P., Toutlemonde, F. "Shear behaviour of ultrahigh performance fiber-reinforced concrete beams. I: Experimental investigation", Journal of Structural Engineering, 140(5), 04013111, 2014. https://doi.org/10.1061/(ASCE)ST.1943-541X.0000907

[28] Țibea, C., Bompa, D. V. "Ultimate shear response of ultra-high-performance steel fibre-reinforced concrete elements", Archives of Civil and Mechanical Engineering, 20(2), 49, 2020. https://doi.org/10.1007/s43452-020-00051-z

[29] Hosamo, H., Sarwari, P. "Experimental and finite element analysis of the shear behaviour of UHPC beams", MSc Thesis, University of Agder, 2019.

[30] Smith, A. S. J., Xu, G. "Simplified and cost-effective method of studying the effect of steel fibers on ultra-high performance concrete specimens' properties/members' performance", Periodica Polytechnica Civil Engineering, 67(1), pp. 308–324, 2023. https://doi.org/10.3311/PPci.20833

[31] Dinh, H. H. "Sear behaviour of steel fiber reinforced concrete beams without stirrup reinforcement", PhD Dissertation, University of Michigan, 2009.

[32] Son, J., Beak, B., Choi, C. "Experimental Study on shear strength for ultra-high performance concrete beam", In: Proceedings of the 18th International Conference on Composites Materials (ICCM-18), Jeju Island, South Korea, 2011, pp. 1–4.

[33] Pillai, S. U., Menon, D. "Reinforced concrete design", McGraw Hill Education, 2003. ISBN 9780070495043

[34] Bahij, S., Adekunle, S. K., Al-Osta, M., Ahmad, S., Al-Dulaijan, S. U., Rahman, M. K. "Numerical investigation of the shear behaviour of reinforced ultra-high-performance concrete beams", Structural Concrete, 19(1), pp. 305–317, 2018. https://doi.org/10.1002/suco.201700062

[35] Aziz, O. Q., Ali, M. H. "Shear strength and behaviour of Ultra-high performance fiber reinforced concrete (UHPC) deep beams without web reinforcement", International Journal of Civil Engineering, 2(3), pp. 85–96, 2013.

[36] Voo, Y. L., Foster, S. J., Gilbert, R. I. "Shear strength of fiber reinforced reactive powder concrete prestressed girders without stirrups", Journal of Advanced Concrete Technology, 4(1), pp. 123–132, 2006. https://doi.org/10.3151/jact.4.123

[37] Baby, F., Marchand, P., Toutlemonde, F. "Shear behaviour of ultra-high performance fiber-reinforced concrete beams. II: Analysis and design provisions", Journal of Structural Engineering, 140(5), 04013112, 2014. https://doi.org/10.1061/(ASCE)ST.1943-541X.0000908

[38] Ueda, T., Sato, Y., Ito, T., Nishizono K. "Shear deformation of reinforced concrete beam", Doboku Gakkai Ronbunshu, 2002(711), pp. 205–215, 2002. https://doi.org/10.2208/jscej.2002.711_205

[39] Bahraq, A. A., Al-Osta, M. A., Ahmad, S., Al-Zahrani, M. M., Al-Dulaijan, S. O., Rahman, M. K. "Experimental and numerical investigation of shear behaviour of RC beams strengthened by ultra-high performance concrete", International Journal of Concrete Structures and Materials, 13(1), 6, 2019. https://doi.org/10.1186/s40069-018-0330-z

[40] Al-Azzawi, A. A., Ali, A. S., Risan, H. K. "Behaviour of ultra-high performance concrete structures", ARPN Journal of Engineering and Applied Sciences, 6(5), pp. 95–109, 2011.

[41] Smith, A. S. J., Sam, J. "Use of correlation and regression analyses as statistical tools in green concrete research", Global Scientific Journal, 8(5), pp. 991–1004, 2020.

[42] Singh, B., Chintakindi, S. "An appraisal of dowel action in reinforced concrete beams", Proceedings of the Institution of Civil Engineers - Structures and Buildings, 166(5), pp. 257–267, 2013. https://doi.org/10.1680/STBU.10.00071

[43] Voo, Y. L., Poon, W. K., Foster, S. J. "Shear strength of fiber-reinforced ultrahigh- performance concrete beams without stirrups", Journal of Structural Engineering, 136(11), pp. 1393–1400, 2010. https://doi.org/10.1061/(ASCE)ST.1943-541X.0000234